Meccanica (2005) 40: 203–219
DOI 10.1007/s11012-005-3067-0
© Springer 2005

Kinematic Model for Determination of Human Arm Reachable Workspace

NIVES KLOPČAR and JADRAN LENARČIČ*
Jožef Stefan Institute, Ljubljana, Slovenia

(Received: 11 September 2004; accepted in revised form: 20 January 2005)

Abstract. In physiotherapy, a standard method to determine the movability and functionality of the human arm is to measure the ranges of motion in joints in sagittal, horizontal and frontal plane. It is clear, however, that these angles can hardly interpret the characteristics of the arm. The main idea in the article is to combine these angles with an adequate kinematic model in order to compute and graphically represent the reachable workspace of the arm, which then serves as an advanced criterion for a more objective evaluation. In this article, we report an improved kinematic model of the human arm which is appropriate for computing and visualizing the human arm reachable workspace. Optical measurements were performed to define the structure and parameters of the model and to develop the mathematical relations between the joint angles. The kinematic model was implemented in a computer programme which is now being introduced in practice and can be used in rehabilitation, ergonomics and sports.

Key words: Human arm, Upper extremity, Kinematic model, Reachable workspace, Rehabilitation evaluation, Computer-aided evaluation.

1. Introduction

The purpose of this investigation is to develop a kinematic model of the human arm which enables us to compute, visualize and quantify the human arm reachable workspace. Here, the reachable workspace is referred to as the volume within which all points can be reached by a chosen reference point on the wrist [11], namely the centre point between process styloideus ulnae and process styloideus radii [12]. The developed kinematic model is implemented in a computer program which is now in the process of being introduced as part of a regular measurement and evaluation procedure in the treatment of patients with shoulder injuries in the national rehabilitation centre.

The input data to the model are the arm dimensions and the ranges of motion in the joints of the shoulder and of the elbow complexes as measured by the physiotherapist. At the current stage, the measurement technique in the rehabilitation centre is entirely manual and only standardized selective motions are measured. The main difficulty, however, is related to the effectiveness of the computation of the workspace from the measured data since this is an extremely time-consuming numerical procedure. To make it useful and implementable on a personal computer, a concise kinematic model of the human upper extremity must be used.

*Author for correspondence: e-mail: jadran.lenarcic@ijs.si

The kinematics of the human arm, in particular of the shoulder complex, had extensively been investigated in the past [4,17,19,3]. However, biomechanical models, which serve to understand the physiology of the arm, are usually too complex to serve in the computation of the arm's reachable workspace. On the other hand, too simple kinematic models, which are usually used in humanoid robotics, do not provide us with enough information [2].

In our investigation, the human arm motion is seen as a combination of the shoulder and the elbow motion. The shoulder motion is composed of elementary motions in the glenohumeral, scapulothoracic, sternoclavicular, and acromioclavicular joint [20]. In order to obtain the reachable workspace effectively, all these motions are modelled as two joints, the inner and the outer shoulder joint. The elbow joint is understood as a uniaxial joint connecting the ulna with the humerus and the radius with the humerus. These two joints allow the elbow flexion and extension [13] and are modelled as a single rotation. The radioulnar joint, which allows the supination and pronation of the forearm, is not included in the model since it does not influence the spatial position of the wrist.

The workspace is computed as a set of points in space that can be reached by the reference point of the hand and is then graphically converted into a three-dimensional body diagram by the use of a computer graphics module. A physiotherapist can utilize this system to compute and visualize the workspace of the injured arm and compare it with an ideal healthy arm. It is possible to numerically quantify the workspace in terms of its volume, compactness and other mathematical criteria representing the arm functionality. In the end of the article, an example of a particular subject is reported and the computed workspace is compared with the measured one.

2. Kinematic Arrangement of Human Arm

The human arm possesses an extremely complicated mechanical structure. It is composed of a skeletal system with several bones, tendons and muscles. They form different combinations of serial and parallel kinematic chains and each joint in the system can possess more than one degree of freedom. The joint motions are mechanically interrelated through the operation of many actuators that drive the same joint and actuators that drive more joints simultaneously.

2.1. Measurement of Principal Human Arm Motions

To monitor and evaluate the human arm motions, the Optotrak optical measurement system was used. This system allowed highly accurate measurement of 3D positions of active markers which were attached to the skin of the measured subjects. The resulting trajectories of markers were numerically processed. Although the applied measurement technique presented several difficulties (most of the problems were related to the deformation of the skin and disappearance of markers during the motion of the arm), it appeared, in connection to well prepared measurement protocols, sufficiently versatile and accurate for the purpose. Figure 1 shows a phase of the measurement of the shoulder girdle. Five male and five female healthy subjects were measured in order to develop the kinematic model of the arm. The age of the

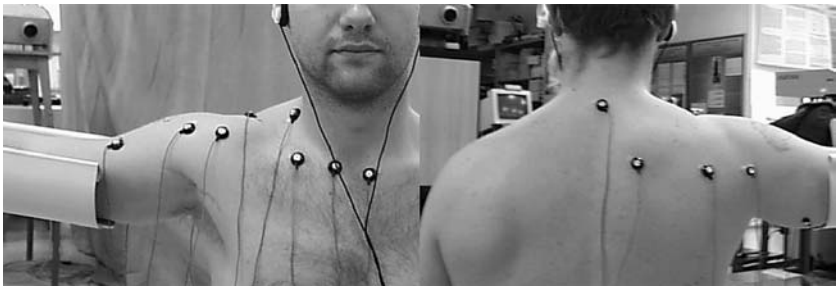

Figure 1. Optoelectrical measurement of shoulder girdle movements.

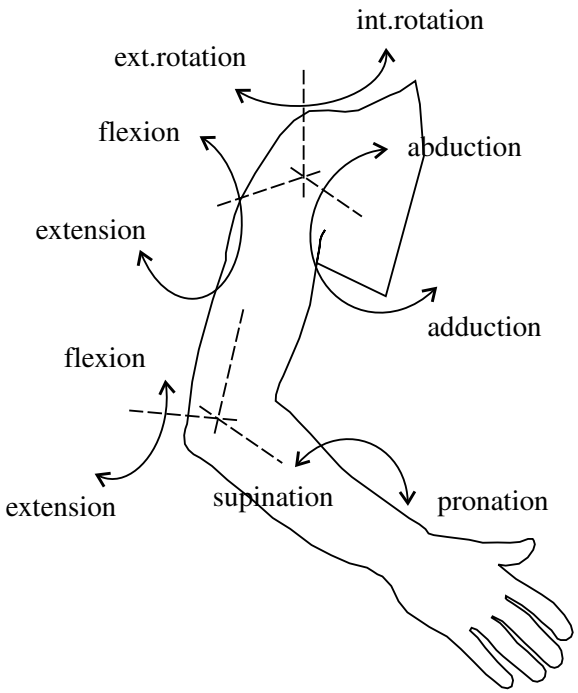

Figure 2. Principal motions of human shoulder and elbow complex.

subjects varied within 24.8 ± 1.4 years. The hight of the male subjects was 1.810 ± 0.030 m and weight 78.0 ± 2.5 kg. The hight of the female subjects was 1.662 ± 0.049 m and weight 50.6 ± 1.7 kg. The repeatability of measurements was within $\pm\pi/36$ radians.

The movements of the arm were measured relative to the chosen reference pose of the limb, which is when the upper arm is fully extended downward by the side of the body and the forearm placed forward in a horizontal direction while the palm of the hand is turned towards the body. The principal shoulder movements are shown in Figure 2. The shoulder elevation through flexion and extension are measured in the sagittal plane around the coronal axis, the elevation through abduction and adduction is measured in the frontal plane around an anterior–posterior axis. The internal and external rotations are measured in the horizontal plane around a vertical axis [16, 10, 15].

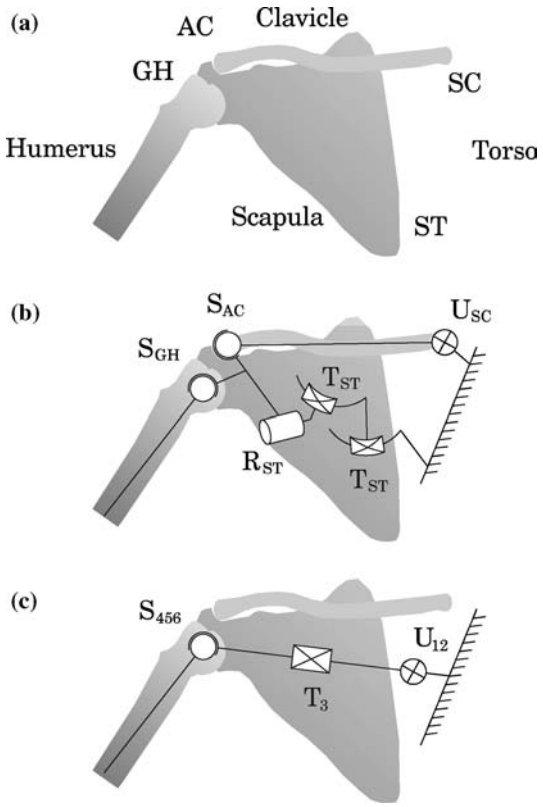

Figure 3. Shoulder kinematic arrangement (frontal view).

The principal elbow movement is the flexion-extension which is measured in the sagittal plane and pronation-supination which is measured about the forearm axis.

2.2. Shoulder Complex

The innermost portion of the shoulder is the shoulder girdle [4, 19, 3]. It consists of two bones, the clavicle and the scapula, which connect the humerus (the upper arm) to the torso (Figure 3). The motion of the girdle is enabled by the scapulothoracic, sternoclavicular, and acromioclavicular joint denoted in Figure 3(**a**) by ST, SC, AC, respectively. The clavicle is attached to the torso through the compound sternoclavicular joint in which the clavicle articulates with the manubrium of the sternum and the cartilage of the first rib [20]. The lateral end of the clavicle is attached to the acromion on the scapula. The sternoclavicular and the acromioclavicular joint can thus be seen as two universal joints separated by an intermediate roll. In Figure 3(**b**), this system is modelled by a universal joint U_{SC} (two rotations) connecting the clavicle to the torso and by a spherical joint S_{AC} (three rotations) connecting the clavicle to the scapula.

The scapulothoracic articulation contains two mating surfaces separated by subscapularis and serratus anterior muscles, which glide over each other during motion. It allows (non-planar) translation and rotatory movement of the scapula with respect to the torso. This non-synovial connection is very compliant due to the layers of

muscles between the scapula and thorax. The motion of the scapula over the thorax has a moving centre which is very difficult to characterize due to the compliance [20]. In a first approximation, we can kinematically model this joint by two sliders T_{ST} and a rotation R_{ST}, each containing one degree of freedom.

Since the bones of the shoulder girdle move conjointly, it can be seen as a parallel mechanism in which the scapula plays the role of the platform and the torso has the role of the base. One leg of this parallel mechanism is the articulation between the scapula and the torso, the other leg is the clavicle. Hence, the total number of degrees of freedom in the joints of the shoulder girdle is $f = 3 + 2 + 1 + 1 + 1 = 8$, where 3 belong to the spherical joint S_{AC}, 2 to the universal joint U_{SC}, and one to translations T_{ST} and rotation R_{ST}. The number of movable segments is $N = 4$ and the number of joints is $n = 5$. In accordance to the Grübler/Kutzbach formula [6] the shoulder girdle thus possesses

$$F_S = \lambda(N - n) + f = 6(4 - 5) + 8 = 2, \tag{1}$$

independent degrees of freedom. Note that $\lambda = 6$ is used since the girdle's motion is considered spatial.

One can see that these two degrees of freedom characterize the motion of the scapula and are mostly rotatory. Such a motion can be modelled by using an universal joint U_{12}, as shown in Figure 3(**c**), combined with a dependent translation T_3 which models the change in length between the torso and the glenohumeral joint. Only the two rotations of the first joint need to be controlled while the translation is dependent on the inclination angles in the first joint [14].

The glenohumeral joint GH attaches the upper arm to the shoulder. It is a ball-and-socket joint (S_{GH}) between the glenoid cavity on the scapula and the head of the humerus. The mating surfaces are quite congruent and have a similar radius. Thus the motion is mostly rotatory. The glenohumeral joint has a wide range of motion because the socket is small and the joint capsule provides little additional support. We can approximate it by three rotations concentrated in a spherical joint S_{456} (Figure 3(c)) with the centre of rotations placed in the centre of the head of the humerus.

The shoulder complex thus contributes to the humerus

$$F_H = 2 + 3 = 5, \tag{2}$$

degrees of freedom. Mechanically, the shoulder complex can be seen as a double pointing-orienting system (a system of a dislocated universal and a spherical joint) enabling a complete orientation of the upper arm [13].

2.3. Elbow Complex

The elbow complex and the forearm is a system of articulations between three bones, which are the ulna, the radius and the humerus (Figure 4(**a**)). The elbow joint is a compound joint consisting of the humeroulnar joint HU and the humeroradial joint HR. The humeroulnar joint HU is a hinge joint between the trochlea of humerus and the trochlear notch of ulna. It allows the ulna to rotate with respect to the humerus. The humeroradial joint HR is a ball-and-socket joint between the capitulum of the

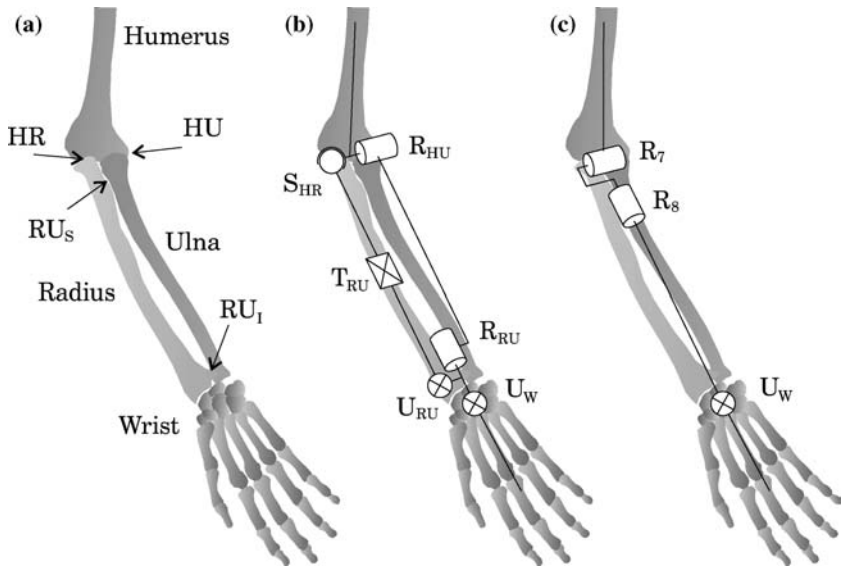

Figure 4. Forearm kinematic arrangement.

humerus and the radial head. The ulna and radius are connected at both ends. The superior (proximal) radioulnar joint RU_S is between the radial head and the radial notch of ulna. The inferior (distal) radioulnar joint RU_I is between the distal ends of the radius and ulna. The radioulnar joints can be seen as pivot joints allowing the radius to rotate about a longitudinal axis the ulna.

The forearm is a parallel mechanism [7] whose mechanical approximation is shown in Figure 4(**b**). Rotation R_{HU} represents the humeroulnar joint which enables the inclination movement of the ulna relative to the humerus, S_{HR} replicates the spherical humeroradial joint, and rotation R_{RU}, translation T_{RU} and universal joint U_{RU} allow the radius to rotate about the ulna. This mechanism contains $N=4$ moving segments, $n=5$ joints, and the sum of degrees of freedom in the included joints is $f=1+1+1+2+3=8$. Here, rotations R_{HU} and R_{RU} and translation T_{RU} contribute 1, universal joint U_{RU} contributes 2, and spherical joint S_{HR} contributes 3 degrees of freedom. In accordance to to the Grübler/Kutzbach formula we can calculate the number of degrees of freedom of this mechanism by

$$F_E=\lambda(N-n)+f=6(4-5)+8=2. \tag{3}$$

These can be replaced by two simple rotations R_7 and R_8 as shown in Figure 4(c). Here, rotation R_7 replicates the elbow flexion extension, and rotation R_8 replicates the pronation supination movement of the forearm. Note that in the human arm the so-called hyperextension is blocked by the olecranon process on the ulna fitting into the olecranon fossa on the humerus.

3. Kinematic Model for Workspace Determination

The structure of the kinematic model used in this investigation is shown in Figure 5. This model enables calculation of the reachable positions of point W which lies between process styloideus ulnae and process styloideus radii. The inner shoulder

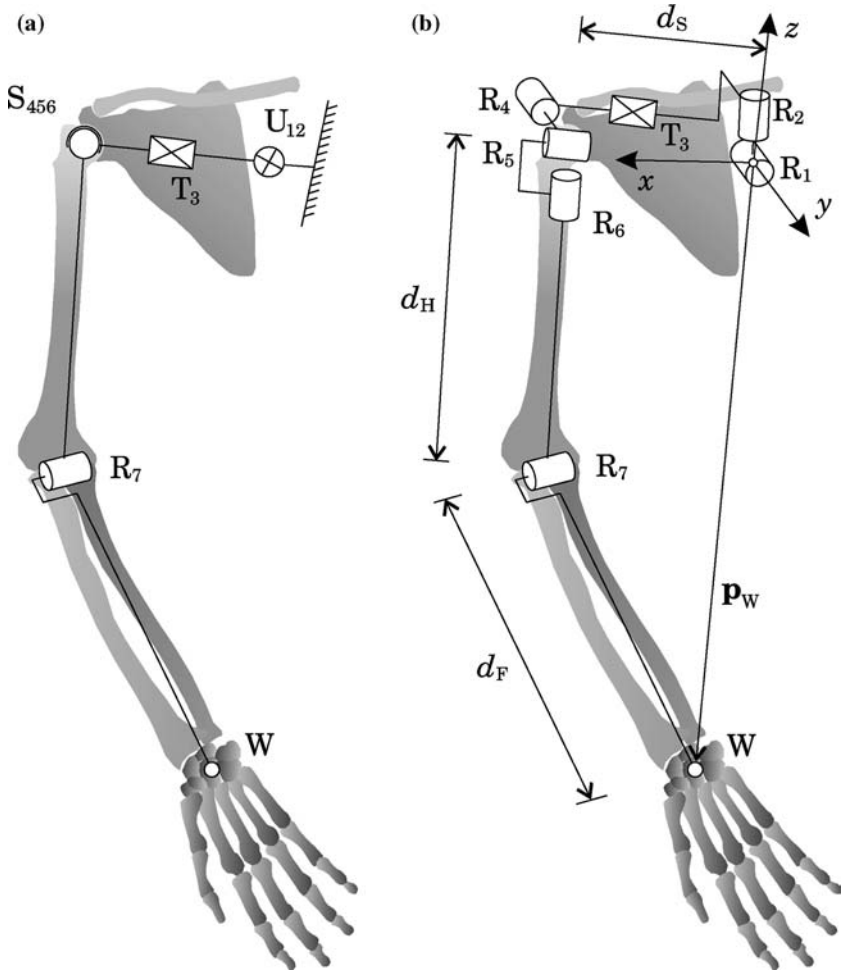

Figure 5. Human arm kinematic model for determination of reachable workspace referred to point W.

joint is universal U_{12}, the outer shoulder joint is spherical S_{456} (Figure 5(**a**)), they are connected by translation T_3, and there is a single rotation R_7 representing the elbow flexion-extension movement. Note that the motion of supination-pronation (R_8 in Figure 4) is left out because it does not influence the position of point W. For the sake of simplicity, the universal joint U_{12} and the spherical joint S_{456} are replaced by a series of rotations intersecting in one point as are shown in Figure 5(**b**). They are R_1, R_2 and R_4, R_5, R_6 for the inner shoulder joint and for the outer shoulder joint, respectively. Note that the outer shoulder joint is positioned in the centre of the glenohumeral joint, while the inner shoulder joint lies on the intersection of an posterior–anterior axis, which passes through the centre of the sternoclavicular joint, and a medial-lateral axis, which passes through the centre of the glenohumeral joint.

3.1. Basic Arm Kinematics

We associate the described degrees of freedom with the anatomical motions of the arm. R_1 represents the elevation–depression of the shoulder girdle, R_2 the

protraction–retraction of the shoulder girdle, R_4 the humeral abduction–adduction, R_5 the humeral flexion-extension, R_6 the humeral internal-external rotation, and R_7 represents the elbow flexion-extension. Translation T_3 does not represent an anatomical motion. It is a dependent joint coordinate which describes the change of the distance between the inner and the outer shoulder joint as a function of other coordinates.

The coordinates of rotations R_1, R_2, R_4, R_5, R_6, R_7 are joint angles q_1, q_2, q_4, q_5, q_6, q_7, respectively. The coordinate of translation T_3 is a linear displacement q_3. Parameter d_S represents the size of the shoulder and is the length between the inner shoulder joint and the outer shoulder joint (when $q_3 = 0$), d_H represents the humerus and is the length between the outer shoulder joint and the elbow joint, d_F represents the forearm and is the length between the elbow joint and reference point W. The reference coordinate frame is attached to the torso in the centre of the inner shoulder joint as shown in Figure 5. In the reference pose of the arm, when all joint coordinates are zero, $q_1, \ldots, q_7 = 0$, R_1 is parallel to y, R_2 is parallel to z, T_3 is parallel to x, R_4 is parallel to y, R_5 is parallel to x, R_6 is parallel to z, and R_7 is parallel to x, while the shoulder link (d_S) is parallel to x, the upper arm link (d_H) is parallel to z, and the forearm link (d_F) is parallel to axis y.

Accordingly, the position of point W with respect to the reference coordinate frame (as shown in Figure 5(b)) can be obtained by

$$\mathbf{p}_W = \mathbf{A}_1\mathbf{A}_2(\mathbf{d}_S + \mathbf{A}_4\mathbf{A}_5\mathbf{A}_6(\mathbf{d}_H + \mathbf{A}_7\mathbf{d}_F)). \tag{4}$$

Here, the following vectors are introduced

$$\mathbf{d}_S = (d_S + q_3, 0, 0)^T, \quad \mathbf{d}_H = (0, 0, -d_H)^T, \quad \mathbf{d}_F = (0, d_F, 0)^T, \tag{5}$$

and $\mathbf{A}_i$ are the following rotation matrices

$$\mathbf{A}_1 = \begin{bmatrix} c_1 & 0 & s_1 \\ 0 & 1 & 0 \\ -s_1 & 0 & c_1 \end{bmatrix}, \quad \mathbf{A}_2 = \begin{bmatrix} c_2 & -s_2 & 0 \\ s_2 & c_2 & 0 \\ 0 & 0 & 1 \end{bmatrix}, \quad \mathbf{A}_4 = \begin{bmatrix} c_4 & 0 & s_4 \\ 0 & 1 & 0 \\ -s_4 & 0 & c_4 \end{bmatrix},$$
$$\mathbf{A}_5 = \begin{bmatrix} 1 & 0 & 0 \\ 0 & c_5 & -s_5 \\ 0 & s_5 & c_5 \end{bmatrix}, \quad \mathbf{A}_6 = \begin{bmatrix} c_6 & -s_6 & 0 \\ s_6 & c_6 & 0 \\ 0 & 0 & 1 \end{bmatrix}, \quad \mathbf{A}_7 = \begin{bmatrix} 1 & 0 & 0 \\ 0 & c_7 & -s_7 \\ 0 & s_7 & c_7 \end{bmatrix}. \tag{6}$$

Here, $s_i = \sin q_i$ and $c_i = \cos q_i$.

3.2. Joint Limits and Interdependencies of Coordinates

To compute the whole set of points $\mathbf{p}_W$ which form the reachable workspace of the arm we also need to determine the minimum and the maximum values of joint coordinates $q_1, \ldots, q_7$. It is, unfortunately, a difficult task because these coordinates cannot directly be measured and because their values are interdependent.

To solve this problem we make use of a simplified kinematic model which replicates standard anatomical motions usually examined in physiotherapy and sports (Figure 2). It includes only three perpendicular revolute joints to describe the motion of the whole shoulder complex, including the glenohumeral joint and the shoulder

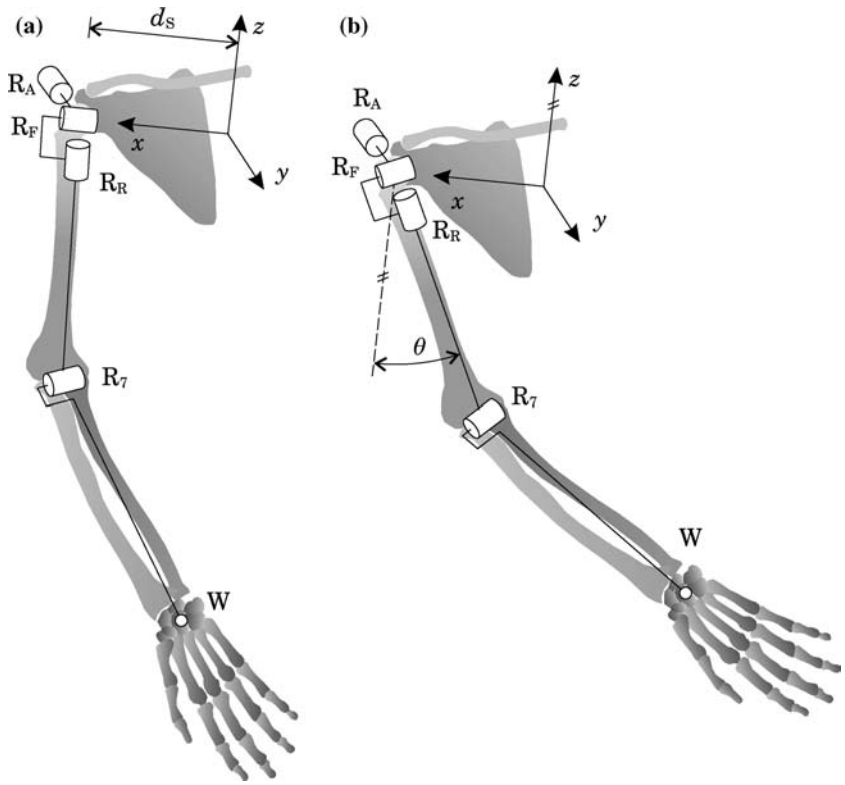

Figure 6. Simplified kinematic model for determination of interrelations between coordinates.

girdle as shown in Figure 6(**a**). Here, R_A is associated with the shoulder abduction-adduction movement, R_F with the shoulder flexion–extension movement, and R_R with the internal–external shoulder rotation. It is clear that R_A, R_F and R_R approximate the movements in both, the inner (R_1, R_2 and T_3) and the outer shoulder joint (R_4, R_5 and R_6) as they are presented in Figure 5. The coordinates of R_A, R_F, R_R are angles θ_A, θ_F, θ_R, respectively, and the associated rotation matrices are

$$\mathbf{A}_A = \begin{bmatrix} c_A & 0 & s_A \\ 0 & 1 & 0 \\ -s_A & 0 & c_A \end{bmatrix}, \quad \mathbf{A}_F = \begin{bmatrix} 1 & 0 & 0 \\ 0 & c_F & -s_F \\ 0 & s_F & c_F \end{bmatrix}, \quad \mathbf{A}_R = \begin{bmatrix} c_R & -s_R & 0 \\ s_R & c_R & 0 \\ 0 & 0 & 1 \end{bmatrix}. \tag{7}$$

Here, $s_X = \sin\theta_X$ and $c_X = \cos\theta_X$.

The ranges of angles θ_A, θ_F, θ_R serve as a standard evaluation criterion in physiotherapy to treat the movability of the arm in sagittal, frontal and horizontal plane and are usually considered as independent of each other. We demonstrated, however, that the range of one angle depends on the current values of the other two [12]. These dependencies were expressed so that the first range is independent of the other two coordinates as follows (all angles are in radians)

$$\theta_A = (\theta_{Am}, \theta_{AM}), \tag{8}$$

where θ_{Am} and θ_{AM} are the lower and the upper limit of angle θ_A measured for a specific person at $\theta_F, \theta_R = 0$. The range of the second joint angle is then dependent on the value of the first one as follows

$$\theta_F = \left(\theta_{Fm} + \frac{1}{3}\theta_A, \theta_{FM} - \frac{1}{6}\theta_A\right), \tag{9}$$

where θ_{Fm} and θ_{FM} are the lower and the upper limit of angle θ_F measured for a specific person at $\theta_A, \theta_R = 0$. Finally, the range of the third joint angle depends on the values of the first two as follows

$$\theta_R = \left(\theta_{Rm} + \frac{7}{9}\theta_A - \frac{1}{9}\theta_F + \frac{4}{9\pi}\theta_A\theta_F, \theta_{RM} + \frac{4}{9}\theta_A - \frac{5}{9}\theta_F + \frac{10}{9\pi}\theta_A\theta_F\right), \tag{10}$$

where θ_{Rm} and θ_{RM} are the lower and the upper limit of angle θ_R measured for a specific person at $\theta_A, \theta_F = 0$. The above relationships were formulated in our previous work [12] and the reachable workspace was then obtained based on the following equation

$$\mathbf{p}'_W = \mathbf{d}'_S + \mathbf{A}_A\mathbf{A}_F\mathbf{A}_R(\mathbf{d}_H + \mathbf{A}_7\mathbf{d}_F), \tag{11}$$

representing the spatial position of point W, where $\mathbf{d}'_S = (d_S, 0, 0)^T$. A clear difference with $\mathbf{p}_W$ (equation (4)) is that $\mathbf{p}'_W$ does not take into account the function of the inner shoulder joint and is, therefore, less accurate.

We observed that we can express the joint limits of the inner shoulder joint R_1, R_2 as functions of the humeral elevation angle θ which is measured between the humeral axis and axis z given in Figure 6(b). For known values of angles θ_A and θ_F we get θ by

$$\cos\theta = \cos\theta_A \cos\theta_F \;\Rightarrow\; \theta = \arccos(\cos\theta_A \cos\theta_F). \tag{12}$$

Based on the performed measurements on female and male subjects we deduced the following dependencies of the joint ranges in the inner shoulder joint on the humeral elevation angle θ

$$q_1 = \left(q_{1m} - \frac{3}{72}\theta + \frac{14}{36\pi}\theta^2, q_{1M} - \frac{1}{36}\theta + \frac{8}{36\pi}\theta^2\right), \tag{13}$$

$$q_2 = \left(q_{2m} + \frac{11}{72}\theta - \frac{8}{36\pi}\theta^2, q_{2M} + \frac{11}{72}\theta - \frac{14}{36\pi}\theta^2\right). \tag{14}$$

They are shown in Figures 7 and 8. In these equations, q_{1m} and q_{1M} are the lower and the upper limit of angle q_1, while q_{2m} and q_{2M} are the lower and the upper limit of angle q_2. They are measured for a specific person when the arm is set in a pose in which all joint angles are zero (except the measured one).

To obtain the limits as functions of θ we, in a first step, analyzed the so-called shoulder rhythm. This is a natural motion of the arm (usually studied in the frontal plane [9,8,1] within which the upper arm link and the shoulder link move conjointly. We believe that the shoulder rhythm is not restricted only to the frontal plane but can also be observed in other planes. Thus, the shoulder rhythm was modelled by a coplanar displacement of the upper arm link and of the shoulder link with a constant (humanoid) ratio between these two displacements [13]. In Figures 7 and 8, the middle curves present angles q_1 and q_2 as functions of θ during the shoulder rhythm.

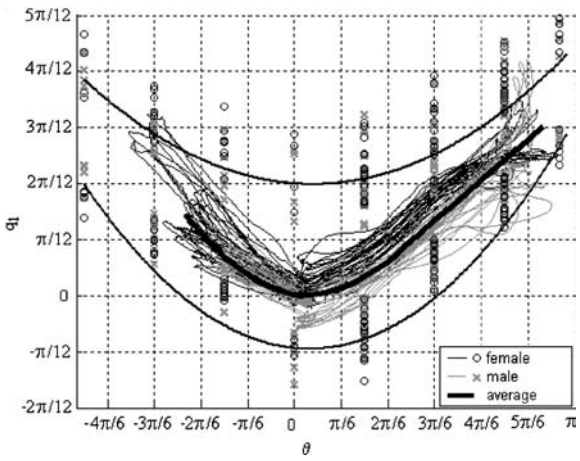

Figure 7. Dependency of range of elevation-depression angle q_1 in inner shoulder joint on humeral elevation angle θ.

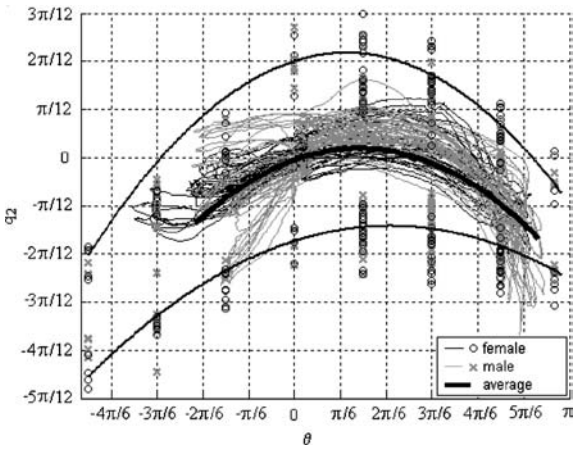

Figure 8. Dependency of range of protraction-retraction angle q_2 in inner shoulder joint on humeral elevation angle θ.

These curves were obtained by using a least-squares method and by imposing a condition that $q_1, q_2 = 0$ when $\theta = 0$. Over this middle curve, in the second step, a maximum and a minimum reach of angles q_1 and q_2 were superimposed. The resultant upper and lower limits are dependent on θ and mathematically expressed in Equation 13 and Equation 14, respectively.

As the principal relationship that connects coordinates $q_1, \ldots, q_6$ (except q_3) with coordinates θ_A, θ_F, θ_R we impose the following

$$\mathbf{A}_1\mathbf{A}_2\mathbf{A}_4\mathbf{A}_5\mathbf{A}_6 = \mathbf{A}_A\mathbf{A}_F\mathbf{A}_R, \tag{15}$$

in which it is required that both sets of revolute coordinates must produce the same orientation of the humerus. This relationship enables us to rewrite the position of point W given in equation (4) in the following way

$$\mathbf{p}_W = \mathbf{A}_1\mathbf{A}_2\mathbf{d}_S + \mathbf{A}_A\mathbf{A}_F\mathbf{A}_R(\mathbf{d}_H + \mathbf{A}_7\mathbf{d}_F). \tag{16}$$

where $\mathbf{p}_W$ is independent of coordinates q_4, q_5, q_6, so that, in extremis, these coordinates are not needed to be known to compute the reachable workspace. However, we might be interested to obtain the values of q_4, q_5, q_6 for other purposes, for example, to deeper understand the properties of the workspace. Let θ_A and θ_F be a known triplet of values which produces an inclination angle θ. Within the limits restricted by this angle we can choose a pair of values q_1 and q_2. Reformulating equation (15) we get

$$\mathbf{A}_4\mathbf{A}_5\mathbf{A}_6 = \mathbf{A}_2^T\mathbf{A}_1^T\mathbf{A}_A\mathbf{A}_F\mathbf{A}_R. \tag{17}$$

Here, the matrices on the right hand side are all known. Their product is a matrix of components a_{ij}. It follows

$$q_4 = \arctan_2 \frac{a_{13}}{a_{33}}, \quad q_5 = -\arcsin a_{23}, \quad q_6 = \arctan_2 \frac{a_{21}}{a_{22}}. \tag{18}$$

And an equivalent solution is

$$q_4' = \arctan_2 \frac{a_{13}}{a_{33}} + \pi, \quad q_5' = \arcsin a_{23} + \pi, \quad q_6' = \arctan_2 \frac{a_{21}}{a_{22}} + \pi. \tag{19}$$

Finally, we observe the value of translation T_3 as a function of θ. The obtained measurements are shown in Figure 9. The middle curve is obtained as a least-squares approximation and is mathematically formulated by

$$\frac{q_3}{d_S} = -\frac{6}{36\pi}\theta^2 + \frac{2}{36\pi}\theta. \tag{20}$$

The range of the elbow joint is considered independent

$$q_7 = (q_{7m}, q_{7M}). \tag{21}$$

Here, q_{7m} and q_{7M} are the lower and the upper limit of angle q_7, which are measured for a specific person.

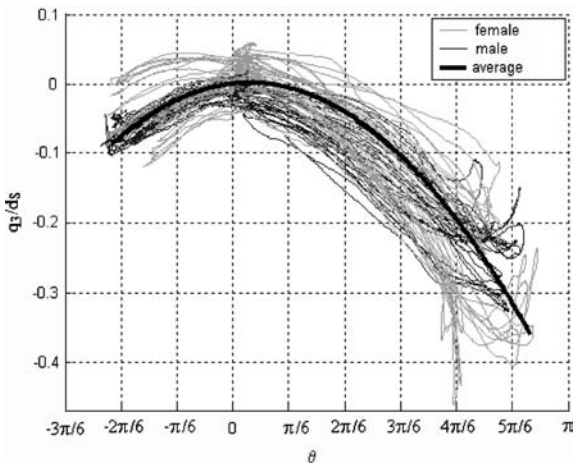

Figure 9. Dependency of relative shoulder girdle length q_3/d_S on humeral elevation angle θ.

4. Workspace Computation and Graphical Representation

The computation of the reachable workspace in our work is based on a set of nested loops within which the values of joint angles are iterated throughout their ranges and the Cartesian vector $\mathbf{p}_W$ is computed in each of these iterations and stored. The procedure is repeated until all ranges of joint angles are swept. In addition, the contacts between the segments of the arm (humerus and forearm) and the body (head, neck and trunk) are taken into account. If during the computation an arm segment intersects the body, the related position of the wrist is eliminated as impossible and is not considered as part of the workspace.

The outer loop is related to coordinate θ_A which is swept throughout a fixed interval in equation (8), where θ_{Am} and θ_{AM} are measured anatomical values pertinent to a specific subject. The next loop is related to coordinate θ_F which is swept throughout a changeable interval in equation (9) and the next loop is related to coordinate θ_R which is swept throughout a changeable interval in equation (10). The input data are the anatomical joint limits measured in the reference pose of the arm, θ_{Am}, θ_{Fm}, θ_{Rm} and θ_{AM}, θ_{FM}, θ_{RM}, which are measured for each specific person. These parameters vary considerably among individuals as they are affected by age, sex, injuries or stage of the illness [16]. The lengths of the arm segments, on the other hand, are computed from the anthropometric table [18] relatively to the subject's height h. This is because physiotherapists do not provide us with this information and also because the variations between individuals are insignificant with respect to the measurement errors in joint angles. Accordingly to the anthropometric table, the length of the shoulder girdle is $d_S = 0.129h$, of the humerus is $d_H = 0.185h$, and of the forearm $d_F = 0.146h$. An elliptical cylinder to approximate the body whose size is $0.174h$ in the frontal plane and $0.089h$ in the sagittal plane is used. The head is approximated by a sphere whose radius is $0.065h$ [18].

For a triplet θ_A, θ_F, θ_R we compute the elevation angle θ accordingly to equation (12) and then two additional loops are introduced, one for coordinate q_1 and one for coordinate q_2. The associated intervals are dependent on angle θ and are described in equations (13) and (14). Here, q_{1m}, q_{2m}, q_{1M}, q_{2M} have to be measured for each individual. Note, however, that these measurements are not standard and must be performed in addition to standard measurement protocols in physiotherapy.

Coordinate q_3 is also a function θ and represents the variable part of the size of the shoulder link. The innermost loop of the workspace computation is related to coordinate q_7. Its values vary inside the independent interval in equation (21), where q_{7m}, q_{7M} are measured. For iteration characterized by a combination of values of θ_A, θ_F, θ_R and q_1, q_2, q_7 the position of point W is computed by equation (16). The result is a cloud of points in Cartesian space representing the insight of the reachable workspace of the arm. To determine the workspace the computation of relative coordinates q_4, q_5, q_6 is not necessary. We might be, however, interested in their values for graphical or other purposes. They can be obtained by equations (18) and (19).

In our computations, the resolution is set to $\pi/36$ for all joint angles. This corresponds to the usual measurement error in the input data as provided to us by physioterapists. Since the ranges of coordinates change from one subject to another and throughout the workspace, it is impossible to exactly predict the number of iterations.

Usually, tens of thousands of iterations are needed to determine the whole set of points approximating the reachable workspace.

The obtained set of points lies inside a cube of edge $L = 2(d_H + d_F)$ whose centre is in the centre of the shoulder joint. This cube is seen as a volume of n^3 smaller cubes with edge L/n, where n is a desired resolution, which is limited by

$$L/n > (d_H + d_F) \tan \frac{\pi}{36}. \tag{22}$$

The cubes that do not contain at least one point $\mathbf{p}_W$ are eliminated. We also eliminate those cubes which are associated with a pose of the upper arm link or the forearm link which interfere with the torso. In the end of this iterative procedure, the workspace of the arm is described by a set of cubes of edge L/n.

In order to increase the accuracy, the cubes forming the surface of the workspace are broken into smaller ones with edge of half length. In every step i the workspace volume is computed by

$$V^i = V_I^i + \frac{V_S^i}{2}, \tag{23}$$

where V_S is the volume of cubes on the surface, and V_I the volume of all other (inner) cubes. The procedure is ended when

$$\nu^i = \frac{|V^i - V^{i-1}|}{V^{i-1}} \tag{24}$$

is smaller than a given value ν. In the end, the surface cubes are smoothed. For this purpose a Bezier interpolation [5] is performed. The workspace can thus be visualized with different colour textures, illuminated with different positions of light, or made transparent.

In Table 1 the measured data of the healthy right arm of a concrete individual are shown. These are the input data to calculate the workspace which is plotted in Figure 10. The hight of the subject was $h = 1.750$ m and the obtained workspace volume was $V = 0.667 \pm 0.055$ m^3. In order to verify the result we superimposed onto the computed workspace in Figure 10 a group of curves measured on the subject representing the maximum reach of the arm (related to the centre of the wrist). The measured curves perfectly matched the computed workspace.

Table 2 shows the measured parameters of the same individual associated with the injured left arm (diaphyseal fracture of the humerus). A comparison of the workspace of the healthy and the workspace of the injured arm is shown in Figure 11. The obtained workspace volume of the injured arm was $V = 0.504 \pm 0.051$ m^3.

Table 1. Measured parameters of healthy right arm (in radians)

θ_{Am}	$-10\pi/180$	θ_{AM}	$170\pi/180$
θ_{Fm}	$-60\pi/180$	θ_{FM}	$170\pi/180$
θ_{Rm}	$-60\pi/180$	θ_{RM}	$90\pi/180$
q_{1m}	$-14\pi/180$	q_{1M}	$30\pi/180$
q_{2m}	$-26\pi/180$	q_{2M}	$30\pi/180$
q_{7m}	$-90\pi/180$	q_{7M}	$60\pi/180$

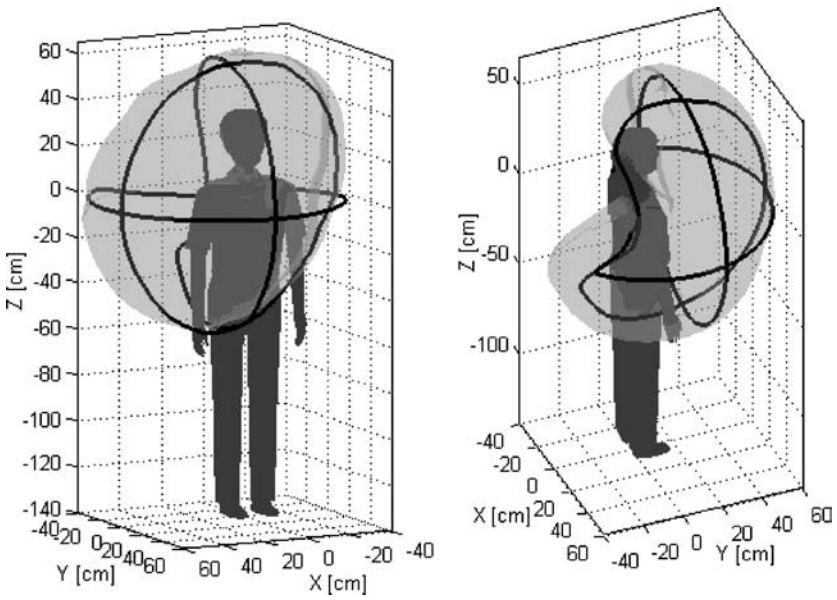

Figure 10. Computed reachable workspace for parameters in Table 1.

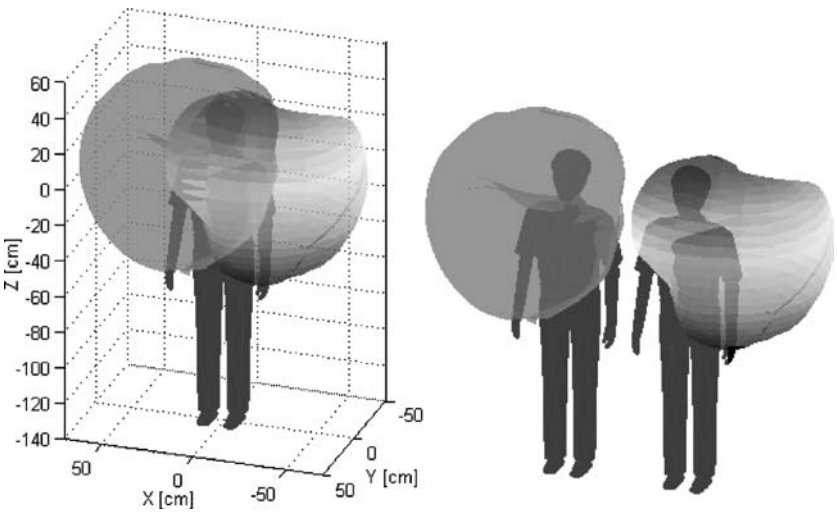

Figure 11. Comparison of computed reachable workspaces for parameters in Table 1 (right arm) and in Table 2 (left arm).

Table 2. Measured parameters of injured left arm (in radians)

θ_{Am}	$-10\pi/180$	θ_{AM}	$170\pi/180$
θ_{Fm}	$-60\pi/180$	θ_{FM}	$135\pi/180$
θ_{Rm}	$-60\pi/180$	θ_{RM}	$75\pi/180$
$q_{1\mathrm{m}}$	$-14\pi/180$	$q_{1\mathrm{M}}$	$30\pi/180$
$q_{2\mathrm{m}}$	$-26\pi/180$	$q_{2\mathrm{M}}$	$30\pi/180$
$q_{7\mathrm{m}}$	$-90\pi/180$	$q_{7\mathrm{M}}$	$60\pi/180$

5. Conclusions

We developed an accurate kinematic model of the human arm with the purpose to compute and visualize its reachable workspace. The model approximates the degrees of freedom in the shoulder girdle, in the glenohumeral joint and in the elbow. In the previous investigations, the human shoulder complex was represented only by a spherical joint (or three perpendicular rotations). Here we improved the model by introducing two eccentric joints, the inner and the outer shoulder joint, representing the function of the shoulder girdle and the function of the glenohumeral joint separately. This double-pointing/orienting system is crucial for replicating the movability of the human arm and its reach can, therefore, be computed in a more accurate way.

Based on a number of measurements on female and male subjects we studied the interdependencies of joint coordinates included in the kinematic model. We observed that the range of motion of one coordinate is dependent on the current values of other joint coordinates. These relationships were expressed in this work in terms of first or second order polynomials.

The developed kinematic model in a first place serves to compute the reachable workspace of the arm which can be used as an evaluation criterion in physiotherapy, ergonomics, rehabilitation and sports. To illustrate the usefulness of the obtained results we computed and plotted the reachable workspace of a concrete person and compared it with some measured curves representing the envelope of the real workspace of this person. In the end, we also showed a comparison between the workspace of the healthy and the workspace of the injured arm of a patient with some shoulder injuries. The kinematic model was implemented in a PC programme which is now being introduced in practice in a rehabilitation centre.

Acknowledgements

The authors are grateful to the Ministry of Education, Science and Sports, Republic of Slovenia, for the support of this investigation.

References

1. Bagg, S.D. and Forrest, W.J., 'Biomechanical model of the human shoulder joint - II. The shoulder rhythm', *J. Biomech.* **67** (1980) 238–245.
2. Benati, M., Gaglio, S., Tagliasco, V. and Zaccaria, R., 'Anthropomorphic robotics', *Biol. Cybern.* **38** (1980) 125–140.
3. Dvir, Z. and Berme, N. 'The shoulder complex in elevation on the arm: a mechanism approach', *J. Biomech.* **11** (1987) 219–225.
4. Engin, A.E. and Tumer, S.T., 'Three-dimensional kinematic modeling of the human shoulder complex – Part I: Physical model and determination of joint sinus cones', *Trans. ASME J. Biomech. Eng.* **111** (1989) 107–112.
5. Gerald, F., *Curves and Surfaces for Computer Aided Geometric Design*, Academic Press Inc. – Harcourt Brace Jovanovich Publisher, 1990.
6. Grübler, M., *Getriebelehre*, Springer-Verlag, Berlin, 1917.
7. Hesselbach, J., Helm, M.B., Kerle, H., Frindt M. and Weinberg, A.M., 'Kinematics of the human forearms pro- and supination', *Advances in Robot Kinematics: Analysis and Control*, Kluwer Academic Publishers, 1998.

8. Högfors, C., Peterson, B., Sigholm, G., Herberts, P., 'Biomechanical model of the human shoulder joint–II. The shoulder rhythm', *J. Biomech.* **24** (1991) 699–709.
9. Inman, V.T., Saunders, J.B. and Abbott L.C., 'Observation on the function of the shoulder joint', *J. Bone Joint Surgery* **26** (1944) 1–30.
10. Kapandji, I.A., *Physiology of the Joints*, Churchill Livingstone, 1970.
11. Kumar, A. and Waldron, K.J., 'The workspace of a mechanical manipulator', *ASME J. Mech. Design* **103** (1981) 665–672.
12. Lenarčič, J. and Umek, A., 'Simple model of human arm reachable workspace', *IEEE Trans. Syst. Man Cyb.* **22** (1994) 1239–1246.
13. Lenarčič, J. and Stanišić, M.M., 'A humanoid shoulder complex and the humeral pointing kinematics', *IEEE Trans. Robotics Automat.* **19** (2003) 499–506.
14. Lenarčič, J., Stanišić, M.M. and Parenti-Castelli, V., 'Kinematic design of a humanoid robotic shoulder complex', In *Proc. Int. Conf. on Robotics and Automat.*, San Francisco, 2000.
15. Magee, D.J., *Orthopaedic Physical Assessment*, 3rd edn. W. B. Saunders Company, 1997.
16. Norkin, C.C. and White, D.J., *Measurement of joint motion: A guide to gonimetry*, F. A. Davis Company Philadelphia, 1985.
17. Tumer, S.T. and Engin, A.E., 'Three-dimensional kinematic modeling of the human shoulder complex–Part II: Mathematical modelling and solution via optimization', *Trans. ASME J. Biomech. Eng.* **111** (1989) 113–121.
18. Winter, D.A., *Bimechanics and Motor Control of Human Movement*, Wiley-Interscience Publication, University of Waterloo, 1990.
19. Wood, J.E., Meek, S.G. and Jacobsen S.C., 'Quantitation of human shoulder anatomy for prosthetic arm control-II. Anatomy Matrices', *J. Biomech.* **22** (1989) 309–325.
20. Zatsiorsky, V.M. *Kinematics of Human Motion*, Human Kinematics, 1998.